

Bouncing water drops

D. RICHARD and D. QUÉRÉ

*Laboratoire de Physique de la Matière Condensée, URA 792 du CNRS
Collège de France - 75231 Paris Cedex 05, France*

(received 8 April 1999; accepted in final form 7 April 2000)

PACS. 68.10.Cr – Surface energy (surface tension, interface tension, angle of contact, etc.).

PACS. 68.45.Gd – Wetting.

PACS. 83.50.Lh – Interfacial and free surface flows; slip.

Abstract. – When a liquid drop impacts a solid, it spreads (with possibly beautiful fingering patterns) up to the point when kinetic energy is dissipated by viscosity. Then, it can retract (if the solid is partially wetted by the liquid), or not. A very different behaviour can be observed on highly hydrophobous solids. On such solids, the contact angle is close to 180° , so that the kinetic energy of the impinging drop can be transferred to surface energy, without spreading. Thus, the drop can fully bounce. However, the liquid nature of this kind of spring imposes a limit for the restitution coefficient, which is due to the fact that the drop, after the lift-off, oscillates.

Full bouncing on a super-hydrophobic substrate. – New substrates of very high hydrophobicity were recently achieved by the Kao group [1–4] and others [5–7]. The idea consists in designing a material associating hydrophobicity and roughness, following the example of what can be observed on some plants [8]. Then, air can be trapped below the drop [7, 9, 10], which leads to contact angles close to 180° with possibly a rather low hysteresis. A water drop deposited on such a solid looks like a pearl.

We studied what happens when a water drop impacts such a surface. The first results are obtained using a substrate (courtesy of V. Coustet, Saint-Gobain) for which the static advancing and receding angles θ_a and θ_r are both of order $170^\circ (\pm 3^\circ)$ and the contact angle hysteresis unappreciable (less than 5°). The advantage of such a surface is to eliminate one of the most natural sources of dissipation, namely the contact angle hysteresis. A water drop ($R = 0.5$ mm) was sent in free fall onto this substrate from a height $H = 2$ cm. The substrate was slightly tilted (angle of order 1°) so that taking a single photograph with a long-time exposure (of order 1 s) reveals the whole trajectory of the drop. Such a picture is displayed in fig. 1.

It is observed that the drop bounces numerous times before coming to rest. The rebound is full, unlike usual splashes which only concern a small fraction of a drop. In the interval between two shocks, the trajectory is parabolic, as expected in the gravity field. Such bounces were reported and qualitatively described for drops impacting pea leaves [11], but what must be stressed here is the remarkable persistence of this behavior (more than 20 shocks): the

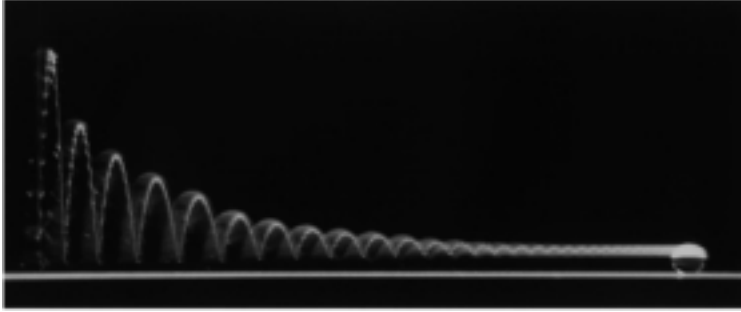


Fig. 1 – Water drop falling on a super-hydrophobic surface ($\theta_a = 170^\circ$) of very small contact angle hysteresis ($\theta_a - \theta_r < 5^\circ$). The drop in motion is illuminated by a continuous lamp which reflects on it, producing a line of light. The plane is slightly tilted (angle of about 1°), which allows us to reveal the whole trajectory of the drop by taking a photograph with a long-time exposure. The vertical scale of the whole picture is 1 cm and the drop diameter 1 mm. A long series of full rebounds is observed. The elasticity is limited by the vibration of the drop after each shock. These vibrations can directly be observed (modulation of the line of light) together with their damping (because of the liquid viscosity) along each parabolic arch. The drop finally stops on the solid, in spite of the slope (even a tiny contact angle hysteresis can be responsible for the sticking of a droplet on an inclined plane).

light line oscillates quite a long time before the drop stops and the height of the last rebound is unappreciable in fig. 1.

The restitution coefficient ε ($\varepsilon = |V'/V|$, where V and V' are, respectively, the velocities before and after the shock) can be measured for each bounce. It is plotted in fig. 2 as a function of the impact velocity V for the experiment of fig. 1 (open circles) and five similar experiments (full circles) done with a slightly smaller drop ($R = 0.4$ mm).

It is observed that the restitution coefficient increases with V at small velocity, which can

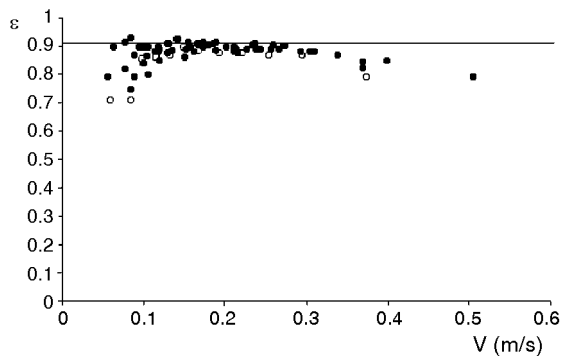


Fig. 2 – Restitution coefficient ε (ratio of the velocities after and before the shock) as a function of the impact velocity V , for each shock in fig. 1 (open circles). The full circles are five series of data obtained on the same substrate with a slightly smaller drop ($R = 0.4$ mm). All these data are below (but close to) the line $\varepsilon = \sqrt{5/6} \approx 0.91$, which is derived in the text. For $V > 0.1$ m/s, the error bars are of order the size of the points; below this value, they significantly increase ($\Delta\varepsilon \sim 0.1$) because it becomes hard to determine (in pictures such as fig. 1) the heights from which the drops are coming.

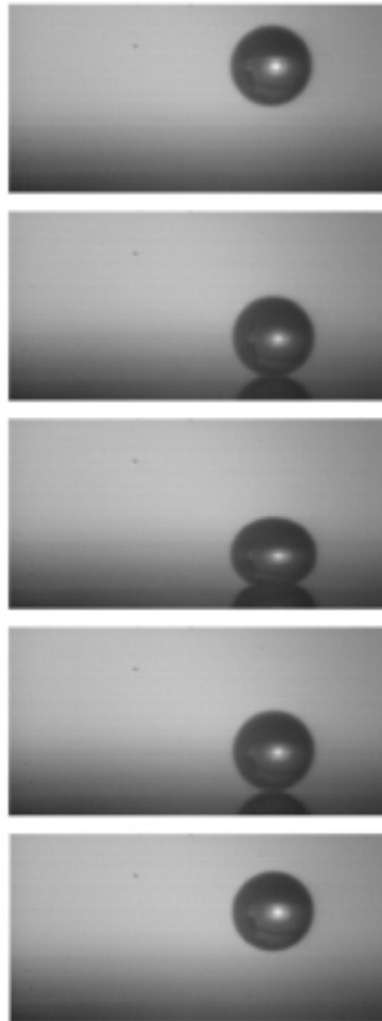


Fig. 3 – Millimetric drop ($R = 0.4$ mm) impacting a super-hydrophobic surface (same as in figs. 1 and 2). The snapshots are obtained thanks to a high-speed camera (9000 frames per second). The liquid is dropped from $H_0 = 0.63$ mm (first picture; $t = -10.8$ ms), hits the surface (second picture; $t = 0$), deforms (third picture, which shows the maximum deformation; $t = 1.1$ ms), lifts off (fourth picture; $t = 2.5$ ms) and rises up to $H_1 = 0.49$ mm (fifth picture; $t = 11.2$ ms). The impact velocity is 11 cm/s and the Weber number 0.07, much smaller than unity. The restitution coefficient deduced from the data is $\varepsilon = 0.88$.

be related to the vicinity of a threshold in velocity for bouncing. Then, ε reaches a maximum and remains quite independent of the impact velocity, in the interval 15 cm/s $< V < 30$ cm/s. Its value is large, of order 0.90, but significantly smaller than 1. At still higher impact velocity, ε slowly decreases with V . Here, we shall mainly focus on the regime of constant ε . We successively discuss the bouncing, and review possible causes of dissipation during the shock.

The shock. – Details of the shock can be obtained thanks to a high-speed camera. The snapshots displayed in fig. 3 were obtained by filming with 9000 frames per second the rebound

of a water drop ($R = 0.4$ mm) on the same substrate as previously. The pictures successively show the drop: i) at the height from which it falls down ($H_0 = 0.63$ mm); ii) as it hits the solid; iii) when it is deformed at most (1.1 ms after the contact); iv) when it lifts off (2.6 ms after the contact); v) when it reaches its highest position after the bouncing ($H_1 = 0.49$ mm). The impact velocity (deduced both from the height and from the movie) is 11.1 cm/s, and the velocity after the shock 9.8 cm/s, which yields $\varepsilon = 0.88$ (the precision of these data is of order 1%).

It is observed that the contact angle remains close to 180° during the whole shock. The drop deforms, so that its kinetic energy can be stored in surface energy. We can define a deformation ratio α for the drop, as the ratio of its largest dimension over its smallest one. At the maximum of deformation, we measure: $\alpha = 1.32 \pm 0.02$. The deformation is light, because we focus on situations where the surface energy of the sphere is larger than the kinetic energy. This condition can be expressed via a dimensionless number, the *Weber number*, which compares both these energies. It writes: $We = \rho V^2 R / \gamma$, noting γ the liquid surface tension and ρ its density. The condition $We \ll 1$ is fulfilled in fig. 3, where we have $We = 0.07$, and more generally in the interval where ε was found to be constant. Another remarkable point is the fact that the drop is spherical as it lifts off: at this point, we measure $\alpha = 1.00 \pm 0.02$.

We can finally estimate the maximum deformation of the drop during the shock. If we approximate its shape in an oblate ellipsoid of great axis $R+x$, the elastic energy stored at this point writes $32\pi/5\gamma x^2$ (it is quadratic in deformation, as for a usual spring). Equating this energy with the kinetic energy of the impinging drop ($E = 1/2MV^2$, M being the drop mass) yields as a maximum deformation $x = \sqrt{5/48RW}e^{1/2}$, from which we recover the condition of small deformation ($x \ll R$ implies $We \ll 1$). We can also deduce the aspect ratio (for an ellipsoid, it is written $\alpha = 1 + 3x/R$). Taking the values corresponding to the experiment in fig. 3 ($We = 0.07$), we find $\alpha = 1.26$ in close agreement with the observed value ($\alpha = 1.3$).

These different features (except the fact that the contact angle remains stuck at its maximum value during the shock) are specific for the limit of small Weber numbers. We have displayed in fig. 4 the maximum extension and the shape at take-off for a millimetric drop impinging the same surface at a much higher velocity ($V = 40$ cm/s, which yields We of order 1). It is indeed observed that the maximum deformation can no longer be approximated by an ellipsoid. Besides, the shape is far from being spherical at lift-off. The drop elongates, all the more since We is larger as observed in fig. 4c. There, the impact velocity is still higher ($V = 80$ cm/s) and the drop larger ($R = 1.8$ mm), which provides a Weber number much higher than 1 ($We = 16$). Then, the drop breaks and emits smaller droplets. These pictures underline *a contrario* the regime we are interested in ($We \ll 1$), where the drop remains intact, and the deformations small.

Dissipation processes. – 1. Most generally, when a drop of liquid hits a solid, it first spreads and forms some kind of a pancake. Then, it possibly retracts or not. Thus, the most natural mechanism for dissipating energy is due to the liquid viscosity η [12]. By contrast, there is no energetic gain to have a spreading stage in a situation of nearly zero wetting, and as we saw, the drop keeps a quasi-spherical shape. Moreover, the contact time of the drop with the solid is very small (of order 2.5 ms, as observed in fig. 3), so that viscous dissipation can be neglected. A crude comparison between the energies dissipated in viscosity and stored in surface tension implies a *Reynolds number* Re ($Re = \rho VR/\eta$), which indeed is much larger than unity (for $V \sim 10$ cm/s, we have $Re \sim 100$). A more careful analysis taking into account the viscous boundary layer developing during the shock would lead to the same conclusion. We finally checked this point by adding some glycerol in the drop, so that the viscosity was

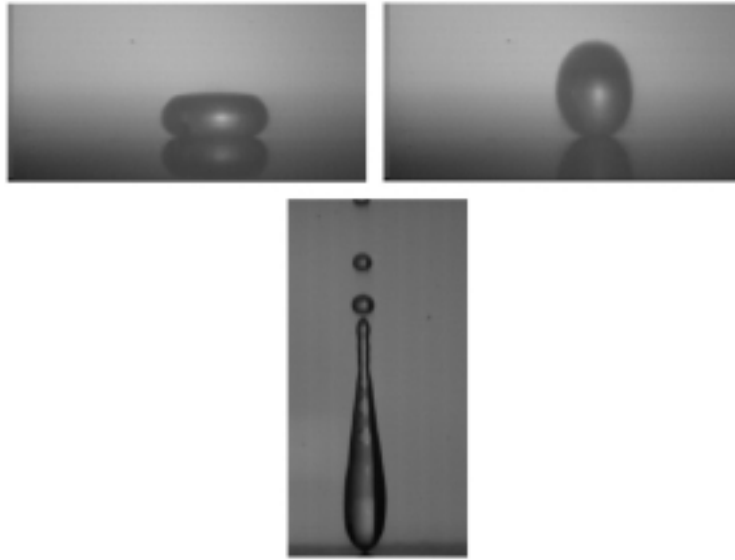


Fig. 4 – Two examples of the deformations which are generated at a Weber number of order 1 or larger (same substrate as previously). In the horizontal pictures, the drop radius is 0.4 mm, the impact velocity 47 cm/s, and We is 1.2, which generates stronger deformations at impact (the drop is no longer close to an ellipsoid) and at lift-off (the drop is far from spherical). At higher We (vertical picture, $We = 18$), a skittle forms at lift-off and emission of droplets is observed: the impact is not full any longer.

doubled: the restitution coefficient was found to remain unchanged in such an experiment.

2. Contact angle hysteresis (CAH) is another natural source of dissipation. Hysteresis is due to the presence of surface defects, and a contact line advancing and receding on such a solid pins and depins on these defects, which induces energy loss. Doing bouncing experiments with a sample of comparable advancing contact angle ($\theta_a = 160^\circ$) but of much higher hysteresis ($\Delta\theta = 30^\circ$) indeed led to less elastic rebounds ($\varepsilon = 0.80$). But, as stressed above, the CAH is very small on the surface we used. Furthermore, it can be observed in fig. 3 (and even 4) that the contact angle remains fixed at its maximum π , which makes the existence of a contact line questionable during the shock (a film of air can remain trapped below the drop). These facts would militate in favour of a negligible influence of the CAH on the restitution coefficient, but a complementary experiment was performed to confirm it.

As it was unlikely to find a liquid-solid system achieving a lower CAH, we used rubber balloons filled with a mixture of water and glycerol: in that case, the elastic membrane plays the role of surface tension. An order of magnitude of this tension can be obtained directly by squeezing the balloons between two plates and measuring the force. One then gets a value of $3 \cdot 10^5$ mN/m for the tension, which yields 15 cm for the capillary length. The static shape of such centimetric balloons was indeed observed to be close to a sphere, as for the drops used above. As another consequence of the very high value for the surface tension, much higher impact velocities can still provide Weber number much smaller than unity: for $R = 4$ cm and $V = 1$ m/s, we find $We = 0.1$.

The results are displayed in fig. 5 for balloons filled with a mixture of water and glycerol 80 times more viscous than water. Though there is no wetting between the impacting object and

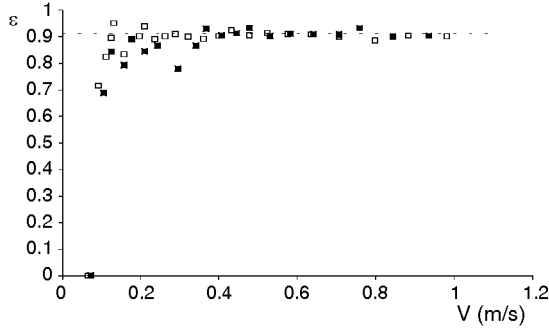


Fig. 5 – Restitution coefficient ε (ratio of the velocities after and before the shock) as a function of the impact velocity V . The full squares are obtained with a balloon of diameter 8 cm and the open ones with a balloon of diameter 4.5 cm. Both were filled with a mixture of water and glycerol of viscosity 80 mPa s. Using balloons allow us to enlarge the scale of the experiment: the surface tension is much higher, so that the impact velocity and the “drop” size can be both larger, while keeping We much smaller than 1. Though there is no contact angle hysteresis in such an experiment, the results are observed to be close to the ones displayed in fig. 2.

the solid surface, we measured in the small deformation regime a constant restitution coefficient close to 0.90, which confirms the negligibility of a capillary sticking in the experiments we made. Note finally that at small impact velocity, the balloon stops bouncing, because of its weight (10^6 larger than the droplet one!). Such transitions between sticking and bouncing will deserve a separate study [13].

3. Thus, even in the *ideal* case of a negligible CAH (figs. 2 and 5), the restitution coefficient was found to be significantly lower than 1, so that a third way for dissipating energy must be envisaged. An important point, not yet discussed, is that *the drop oscillates* after the lift-off, whereas it was just in translation before the impact. Thus, a part of the translational kinetic energy is transferred into internal modes of vibration during the shock. These vibrations are clearly visible in fig. 1, where the line of light is modulated after each shock. It is also observed that the oscillations are damped against time, because of the liquid viscosity (a condition for observing a constant ε all along the series of impact). While viscous dissipation could be neglected during the very short time of impact (of order 1 ms), this cannot be done in the long interval (of order 100 ms) between two shocks where many oscillations occur. The time scale for damping the oscillations in air scales as $\rho R^2/\eta$, and is practically a fraction of a second for millimetric water drops. In the case of much larger liquid balloons presented above, the liquid was taken more viscous to keep the damping time smaller than the typical interval between shocks.

Since the shape at the instant of take-off is spherical, the existence of oscillations show that the velocity field inside the drop is non-homogeneous when it leaves the surface. The existence of such velocity gradients was shown numerically by Fukai for conventional drop impacts [14]. To get an idea on the restitution coefficient it generates, let us take a linear approximation for the velocity field $v(z)$ inside the drop when lifting off: $v(z) = V'z/R$, z being the vertical distance to the solid surface. Since V' is also the speed of the center of mass, the restitution coefficient ($\varepsilon = V'/V$) can finally be deduced by writing the conservation of kinetic energy between the impact ($1/2MV^2$) and the bouncing ($\int_0^{2R} -1/2dMv^2(z)$). We took for the calculation the linear form for $v(z)$ written above, but had also to specify the way the drop mass is spread along the vertical axis at lift-off. If the drop is very elongated (liquid

column), we find $\varepsilon = \sqrt{3}/2$ (about 0.85). If it is spherical (which is indeed the case at small We ; see fig. 3), integration of mass elements yields $\varepsilon = \sqrt{5/6}$ (about 0.91). The latter value is reported in figs. 2 and 5. The very close agreement with the upper limit of ε measured experimentally may be coincidental, since the choice of a linear velocity field during the shock can be questioned. Nevertheless, two important features are explained with this argument, which are the independence of the restitution coefficient from the impact speed and the order of magnitude of the energy loss.

Conclusion. – We have shown that a water drop can fully bounce, as a balloon, when impinging a super-hydrophobic surface. We were interested in the elasticity of this shock, and found that even in an ideal case (small impact velocity, surface of negligible contact angle hysteresis), there was a limit in elasticity, due to the transfer of a part of the kinetic energy into drop vibrations. Details about the shock itself would provide a useful complement to this study: it would be worth studying the nature of the interface between the solid and the liquid (possible existence of a film of air, characterisation of the penetration of the drop inside the porous structure of the solid, etc.) and to measure directly the velocity gradient inside the drop. The latter point should also deserve a careful theoretical approach, together with a comprehension of the dissipation mechanisms for a substrate of appreciable contact angle hysteresis. Finally, extensions to higher Weber numbers for which break-up of the liquid drop is observed would also be very useful, particularly from the viewpoint of practical applications (achievement of so-called water-repellent surfaces).

* * *

We thank V. COUSTET (Saint-Gobain) for putting her super-hydrophobic surface at our disposal and J. BICO, C. CLANET, P.G. DE GENNES and L. MAHADEVAN for discussions and encouragement.

REFERENCES

- [1] ONDA T., SHIBUICHI S., SATOH N. and TSUJII K., *Langmuir*, **12** (1996) 2125.
- [2] SHIBUICHI S., ONDA T., SATOH N. and TSUJII K. J., *Phys. Chem.*, **100** (1996) 19512.
- [3] TSUJII K., YAMAMOTO T., ONDA T. and SHIBUICHI S., *Angew. Chem. Int. Ed. Engl.*, **36** (1997) 1011.
- [4] SHIBUICHI S., YAMAMOTO T., ONDA T. and TSUJII K., *J. Colloid Interface Sci.*, **208** (1998) 287.
- [5] TADANAGA K., KATATA N. and MINAMI T., *J. Am. Ceram. Soc.*, **80** (1997) 1040.
- [6] COUSTET V. and DELATTRE L., unpublished data.
- [7] BICO J., MARZOLIN C. and QUÉRÉ D., *Europhys. Lett.*, **47** (1999) 220.
- [8] NEINHUIS C. and BARTHLOTT W., *Ann. Bot.*, **79** (1997) 667.
- [9] BARTHLOTT W. and NEINHUIS C., *Planta*, **202** (1997) 1.
- [10] JOHNSON R. E. and DETTRE R. H., in *Contact Angle, Wettability and Adhesion*, *Adv. Chem. Ser.*, **43** (1964) 112.
- [11] HARTLEY G. S. and BRUNSKILL R. T., in *Surface Phenomena in Chemistry and Biology*, edited by J. F. DANIELLI (Pergamon Press, London) 1958, pp. 214-223. In this paper, it is indeed reported that a drop can bounce on a leaf, but the characteristics of the shock are not described (in particular, the restitution coefficient). Besides, it is claimed that a large impact velocity is necessary for bouncing to occur, which is clearly not the case in fig. 1.
- [12] REIN M., *Fluid Dyn. Res.*, **12** (1993) 61, and references therein.
- [13] RICHARD D., CLANET C. and QUÉRÉ D., to be published.
- [14] FUKAI J. *et al.*, *Phys. Fluids*, **5** (1993) 2588.